HHS Public Access

Author manuscript

Nature. Author manuscript; available in PMC 2010 April 22.

Published in final edited form as:

Nature. 2009 October 22; 461(7267): 1126–1129. doi:10.1038/nature08487.

The Postsynaptic Function of Type II Cochlear Afferents

Catherine Weisz[1], **Elisabeth Glowatzki**, and **Paul Fuchs**

[1]The Department of Otolaryngology- Head and Neck Surgery, the Department of Neuroscience, The Center for Hearing and Balance and the Center for Sensory Biology, Johns Hopkins University School of Medicine

Abstract

The mammalian cochlea is innervated by two classes of sensory neurons. Type I neurons make up 90-95% of the cochlear nerve and contact single inner hair cells (IHCs) to provide acoustic analysis as we know it. In contrast, the far less numerous Type II neurons arborize extensively among outer hair cells (OHCs) 1,2 and supporting cells3,4. Their scarcity, and smaller caliber axons, have made them the subject of much speculation, but little experimental progress for the past 50 years. Here we record from Type II fibers near their terminal arbors under OHCs to show that these receive excitatory glutamatergic synaptic input. The Type II peripheral arbor conducts action potentials, but the small and infrequent glutamatergic excitation implies a requirement for strong acoustic stimulation. Further, we show that Type II neurons are excited by adenosine tri-phosphate (ATP). Exogenous ATP depolarized Type II neurons both directly, and by evoking glutamatergic synaptic input 5. The present results prove that Type II neurons function as cochlear afferents, and can be modulated by ATP. The lesser magnitude of synaptic drive dictates a fundamentally different role in auditory signaling from that of Type I afferents.

The organ of Corti was dissected from the apical turn of postnatal (P5-19) rat cochleas and secured in a recording chamber. A few OHCs were removed by aspiration to reveal nerve fibers (~2 microns diameter) running along the cochlear spiral (Fig. 1a-c). Gigaohm-seal ruptured-patch recordings were performed from the fibers (Fig. 1a-c). AlexaFluor 488 hydrazide was included in the recording pipette for subsequent visualization via *posthoc* immunolabeling (Fig. 1d). Tracings from two fills (Fig. 1e) show the minimally-branched terminal field several hundred microns basal to a marked right-angle turn in the fiber toward the tunnel of Corti. These fills (in 6 fibers) revealed spiral processes 100-325 microns long that terminated among the OHCs, and variable filling of the radial, central-going process (Supplementary Table 1), in one case to its soma in the spiral ganglion (Fig. 1e). These morphological features accord with Type II afferent innervation patterns 2,6.

Correspondence and requests for materials should be addressed to P. Fuchs (pfuchs1@jhmi.edu)..

Author Contributions: C. Weisz performed and analyzed all experiments with additional analysis from P. Fuchs and E. Glowatzki. C. Weisz, E. Glowatzki and P. Fuchs conceived the project, designed and discussed the experiments, and wrote the paper.

Supplementary Information is linked to the online version of the paper at www.nature.com/nature

Voltage-gated currents were elicited with a series of 10 mV steps from −110 to +30 mV (Fig. 1f). Positive to −60 mV, transient, tetrodotoxin-sensitive inward currents were evoked (Fig. 1f - inset). Based on their all-or-none appearance, these are likely to be 'action currents' arising in distant, un-clamped membrane. Positive to −50 mV sustained outward currents also were evoked. These were not characterized further, except to note that they were reduced when cesium substituted for potassium in the recording pipette.

In current-clamp recording, action potentials were evoked when Type II fibers were depolarized with injected current (Fig. 1g). Small excitatory postsynaptic potentials (EPSPs) were observed that averaged 3.8 ± 2.0 mV in amplitude (n=1709 EPSPs, n=8 fibers).

Under voltage-clamp, excitatory postsynaptic currents (EPSCs) (Fig. 2a and inset) occurred several times per minute under resting conditions. When external potassium was elevated from the normal 5.8 to 15 or 40 mM to depolarize presynaptic sources, EPSC frequency increased (Fig. 2a, Supplementary Table 2). Amplitude histograms typically peaked near 18 pA (holding potential −90 mV) and were slightly skewed toward larger amplitudes (Fig. 2b), reaching a maximum of ~100 pA in some fibers. The mean amplitude value from 30 fibers was 28.3 ± 8.3 pA.

Synaptic currents recorded at different holding potentials were averaged (Fig. 2c) to provide an I-V relation that reversed at 0 mV (n=6 fibers) (Fig. 2d). The AMPA-type glutamate receptor antagonist NBQX reversibly blocked the EPSCs (n=7 fibers) (Fig. 2e). Synaptic currents in Type II fibers were essentially eliminated by nifedipine (n=4) (Fig. 2f) that blocks voltage-gated $Ca_V1.3$ calcium channels in OHCs 7. Thus, EPSCs recorded from Type II fibers are mediated by AMPA-type glutamatergic receptors, and are presumed to reflect transmitter release from OHCs.

Analysis of 12,043 EPSCs in 30 fibers from all rows gave average rise times of 1.1 ± 0.3 ms, and decay time constants of 3.2 ± 1.1 ms at room temperature (Supplementary Table 2, 3). Since each Type II recording site might be anywhere within one length constant of presumptive inputs (Legend, Supplementary Table 1), synaptic waveforms could be altered by cable loss. There was a weak negative correlation between EPSC amplitude and time course in some fibers (Fig. 2g) while others were dominated by kinetically uniform EPSCs (Fig. 2h), as though cable effects varied between recordings. Among 30 fibers there was a significant correlation between average EPSC amplitude and decay time (Fig. 2i), suggesting that recording sites were located at different distances from the synaptic inputs. While Type II EPSCs varied in amplitude and kinetics (Fig. 2j), these typically rose and fell smoothly, without the obvious inflections commonly found in all Type I fiber recordings8.

It is known that OHCs are depolarized by ATP5 and that antibodies to P2X ATP receptors label Type II fibers9. Thus, we next asked whether Type II fibers were affected by ATP. The effect of ATP varied with postnatal age and will be described first for young (P5-9) fibers. ATP applied from a nearby perfusion pipette led to frequent EPSCs (Fig. 3a). ATP evoked EPSCs at 2.4 ± 2.1 /s (n=10 fibers), not significantly different from the effect of 40 mM K^+ that depolarizes OHCs to −35 mV (n=5 fibers) (Supplementary Table 2). ATP also evoked a prolonged inward current in Type II fibers (Fig. 3a). The slow inward current appears to be a

direct effect of ATP on the Type II fiber since it preceded the EPSCs and was unchanged by application of nifedipine that eliminated the ATP-evoked increase in EPSCs (n=4, not shown). In current-clamp experiments ATP depolarized Type II fibers (31.3 ± 10.1 mV, n=4), and induced EPSPs, although action potentials were rarely seen. However, this lack of action potentials may be an artifact of 'wash-out' since ATP reliably induced action potentials in Type II fibers in extracellular, loose-patch recordings (n=7) (Fig. 3b). This excitation was prevented by the P2X antagonist PPADS (n=4, Fig. 3b). PPADS also eliminated ATP-evoked EPSCs observed during intracellular recording from Type II fibers (not shown).

In newly hearing animals (P12-13), Type II fibers had voltage-gated sodium and potassium currents, and EPSCs whose average amplitude and waveform were not different from those of younger fibers (not shown). ATP produced significantly less effect in voltage-clamp (Fig. 3c) and current–clamp (Fig. 3d). However, ATP still was able to evoke extracellularly-recorded action potentials from four of seven Type II fibers at P13. Intracellular fiber recordings become exceedingly difficult with increasing animal age. Nonetheless, voltage-clamp and current-clamp recordings were achieved from several Type II fibers at P17-19, revealing EPSCs (Fig. 3e) and action currents as in younger fibers. In three of six recordings, application of ATP produced an effect on membrane current or membrane potential (Fig. 3f, g), although smaller than at younger ages.

Type II afferent function has been a mystery since the early 20th century 6. In contrast to the wealth of information on Type I afferents, only one anatomically-confirmed Type II recording has been made *in vivo*, showing no spontaneous activity and no response to even very loud sound10. Voltage- and current-clamp recordings from Type II neuronal somata *ex vivo* have begun to define voltage-gated conductances 11, and revealed slowly accommodating repetitive action potentials 12, but could not assess synaptic inputs. By recording near the terminal arbor, we show that Type II afferents receive glutamatergic synaptic input and also are subject to purinergic activation.

The EPSCs in Type II afferents were much less frequent, somewhat slower on average and significantly smaller than glutamatergic EPSCs in Type I afferent boutons on IHCs 8,13. Cable loss is likely to account for some differences in waveform, although other reports suggest the possibility of fundamental differences between Type II and Type I glutamatergic mechanisms 14,15,. What is more certain is that presynaptic mechanisms differ substantially for Type I and Type II afferents. Considering that there are more than a dozen presynaptic OHCs1, EPSCs were remarkably infrequent in Type II afferents compared to much higher release rates from a single IHC ribbon synapse onto a Type I afferent8 (Supplementary Table 2). This implies that overall synaptic transfer is relatively poor from OHCs, consistent with reports of smaller voltage-gated calcium currents in OHCs than in IHCs 16. However, OHCs are capable of vesicular fusion 17, and support it with the same dihydropyridine-sensitive calcium channels ($Ca_V1.3$) as in IHCs 7. Furthermore, OHCs do have synaptic ribbons, though fewer than IHCs, not at every afferent contact, and their prevalence may differ between species 18,19. While Type II afferents also contact Deiters' and Hensen cells these are unlikely to contribute since they possess no presynaptic ultrastructure, and are described as postsynaptic to Type II afferents20,21.

Although Type II synaptic organization remains incompletely resolved, it is clear from the present data that OHCs release vesicles infrequently, and the postsynaptic effect is relatively small. The dominant mode of EPSC amplitude distributions may correspond to the release of a single vesicle, in contrast to multivesicular release at the IHC afferent synapse8,22. In keeping with that suggestion, 'multiphasic' EPSCs were not observed in the Type II recordings, promising future insights into variation among hair cell release mechanisms. Whatever the underlying mechanism, the net result is that synaptic release from OHCs produced only modest depolarization of the Type II fiber, and seems unlikely on its own to signal moderate acoustic stimulation. Although both groups of afferents project together to the cochlear nucleus23, the basalward spiral of Type II afferents implies an offset (~ ¼ octave) toward higher acoustic frequencies than those of associated Type I afferents 4. The present results require such higher frequency sound to be significantly louder, if Type II activity were to be integrated centrally with that of neighboring Type I afferents.

Diverse roles have been suggested for the function of Type II afferents, including measuring the "set-point" of OHC electromotility11, or regulating a local network of signaling between OHCs through reciprocal synapses 14. The developmental fall in sensitivity to ATP observed here is consistent with the down-regulation of some P2X receptors during development24, and suggests a possible role in synaptic maturation like that reported for Type I afferents25. Finally, previous workers have proposed that Type II afferents might mediate responses to loud, even painful sounds 26. Tissue damage triggers calcium waves in supporting cells that depend on release of ATP27, and loud sound can increase ATP levels in cochlear fluids28, reminiscent of the role of ATP in somatic pain29. The participation of Type II afferents would be strengthened by renewed sensitivity to ATP, and there is evidence that exposure to loud sound increases the expression of cochlear P2X receptors 30.

Methods Summary

The organ of Corti was dissected from the apical turn of postnatal (P5-19) rat cochleas and secured in a recording chamber. Four to six outer hair cells (OHCs) were removed by aspiration to reveal nerve fibers (~2 microns diameter) running along the cochlear spiral. Gigaohm-seal ruptured-patch recordings were performed from the fibers using borosilicate glass electrodes with resistances of 6 to 10 MΩ. EPSCs were recorded in voltage-clamp at a membrane holding potential of −90 mV, unless otherwise noted. EPSPs were recorded in current-clamp with the fiber membrane potential held at −60 to −65 mV by direct current injection. Action potentials were induced in current-clamp by depolarizing current injection in 10 pA steps. Action potentials were also recorded during loose-patch extracellular recordings performed with a seal resistance of 3-4 times the electrode resistance. Pharmacological compounds were applied with a gravity-fed, large bore application pipette placed near the recording site. AlexaFluor 488 hydrazide (10 μM) was included in the recording pipette for diffusion into the fiber and subsequent visualization via *posthoc* immunolabeling. The labeled fiber was imaged using a confocal microscope. Data is presented as the mean ± standard deviation.

Methods

Electrophysiological Recordings from Type II Afferents

Sprague-Dawley rat pups (Charles River, Wilmington, MA) of postnatal day 5 through 19 (P5-19) were anesthetized with 0.45 mg/10 g Euthasol (Virbac AH, Inc, Fort Worth, TX) or Isofluorane (Vedco, Inc, Saint Joseph, MO) according to approved Johns Hopkins IACUC guidelines. After ensuring deep anesthesia with a foot pinch, the animals were decapitated, and the temporal bone containing auditory and vestibular peripheral organs was removed. The bone surrounding the cochlea was dissected away and the apical turn of the cochlear spiral was severed at the modiolus. The stria vascularis and tectorial membrane were removed. The entire cochlear turn including spiral ganglion and organ of Corti was mounted under an insect pin glued to a coverslip for electrophysiological experiments.

Standard gigaohm whole cell patch-clamp and loose-patch techniques were employed to record from terminals of the Type II afferent fibers under outer hair cells (OHCs). Using DIC (differential interference contrast) optics, 4-6 OHCs were aspirated to expose the Type II dendrites for giga-ohm seal voltage-clamp recording. Extracellular solution was perfused through the recording chamber at a rate of 2-3 ml / min. The solution contained (in mM): 5.8 potassium chloride, 155 sodium chloride, 1.3 calcium chloride, 0.9 magnesium chloride, 0.7 sodium phosphate, 5.6 glucose, 10 HEPES, pH 7.4. Intracellular solution contained (in mM): 150 potassium chloride, 0.1 calcium chloride, 3.5 magnesium chloride, 5 EGTA, 5 HEPES, 2.5 sodium-ATP, pH 7.2. Chemicals were purchased from Sigma (St Louis, MO). In some experiments ATP was excluded from the intracellular solution or potassium was replaced with cesium chloride. 1 mm borosilicate glass pipettes (WPI, Sarasota, FL) were Sylgard-coated (Corning, Midland, MI) and fire-polished to resistances of 6 to 10 MΩ. All pharmacological compounds were from Tocris Bioscience (Ellisville, MO) unless otherwise stated. Doses used were the following: 50 μM PPADS, 50 μM nifedipine, 10 μM NBQX, 1 - 50 μM ATP. Pharmacological compounds were applied with a large bore pipette positioned near the recording site. Recordings were performed using an Axopatch 200B amplifier (Axon Instruments, Foster City, CA), pClamp version 9.2 (Axon Instruments) and a Digidata 1322A board (Axon). Data were sampled at 50 kHz and low-pass filtered at 10 kHz. Input resistances averaged 550 MΩ, series resistances were on average 25.5 MΩ and were not corrected for. Membrane holding potential is given without liquid junction potential correction of −4 mV. Loose patch extracellular recordings were performed with a seal resistance 3-4 times the pipette resistance.

Data Analysis

EPSCs were analyzed with MiniAnalysis software (Synaptosoft, Decatur, GA) or Clampfit 9.2 (Axon Instruments). Figures were prepared in Origin 8.0 (Origin Labs, Northampton, MA) and Illustrator (Adobe, San Jose, CA). Statistical analysis was performed with JMP (SAS, Cary, NC). All data given as mean ± standard deviation.

Immunohistochemical Enhancement of Neuronal Tracer

The fluorescent neuronal tracer AlexaFluor 488 hydrazide (Molecular Probes, Eugene, OR) was included in the recording pipette at 10 μM. Following recording, cochlear turns were

fixed with 4% paraformaldeyde in phosphate buffered saline (PBS) at pH 7.4 for 60 minutes. The tracer signal was enhanced by immunolabeling with anti-Alexa 488 antibody as follows: block 2 hours at room temperature in 5% normal goat serum with 0.25% Triton X-100 in 60 mM PBS, incubate in primary antibody overnight at 4°C (rabbit anti-Alexa 488, 1:1000 in blocking buffer), rinse 3 × 10 minutes in blocking buffer, incubate in secondary antibody 2 hours at room temperature (goat anti-rabbit 1:2000 in blocking buffer), rinse 1 × 10 minutes in 60 mM PBS, incubate with DAPI nuclear stain (1:1000 in dH_2O), rinse 2 × 10 minutes 60 mM PBS, mount in FlourSave medium (Calbiochem, San Diego, CA).

Equipment and Settings for Digital Images

Cochlear explants were viewed for electrophysiological experiments under a Axioscope microscope (Zeiss, Oberkochen, Germany) using differential interference contrast (DIC) using a 40x water immersion objective and a camera with contrast enhancement (Hamamatsu C2400-07, Hamamatsu City, Japan). Images were collected using a Zeiss LSM 510 Meta confocal microscope. Labeled fibers were measured (LSM Image Browser). Tiled images were traced in Photoshop (Adobe).

Supplementary Material

Refer to Web version on PubMed Central for supplementary material.

Acknowledgements

Supported by NIDCD grants R01 DC000276 and R01 DC006476, T32 DC000023 and a grant from the Blaustein Pain Foundation of Johns Hopkins.

Bibliography

1. Perkins RE, Morest DK. A study of cochlear innervation patterns in cats and rats with the Golgi method and Nomarkski Optics. J Comp Neurol. 1975; 163:129–58. [PubMed: 1100684]
2. Berglund AM, Ryugo DK. Hair cell innervation by spiral ganglion neurons in the mouse. J Comp Neurol. 1987; 255:560–70. [PubMed: 3819031]
3. Fechner FP, Nadol JJ, Burgess BJ, Brown MC. Innervation of supporting cells in the apical turns of the guinea pig cochlea is from type II afferent fibers. J Comp Neurol. 2001; 429:289–98. [PubMed: 11116221]
4. Brown MC. Morphology of labeled afferent fibers in the guinea pig cochlea. J Comp Neurol. 1987; 260:591–604. [PubMed: 3611412]
5. Nakagawa T, Akaike N, Kimitsuki T, Komune S, Arima T. ATP-induced current in isolated outer hair cells of guinea pig cochlea. J Neurophysiol. 1990; 63:1068–74. [PubMed: 2358862]
6. Lorente de No R. The sensory endings in the cochlea. Laryngoscope. 1937; 47:373–377.
7. Michna M, et al. Cav1.3 (alpha1D) Ca^{2+} currents in neonatal outer hair cells of mice. J Physiol. 2003; 553:747–58. [PubMed: 14514878]
8. Glowatzki E, Fuchs PA. Transmitter release at the hair cell ribbon synapse. Nat Neurosci. 2002; 5:147–54. [PubMed: 11802170]
9. Jarlebark LE, Housley GD, Thorne PR. Immunohistochemical localization of adenosine 5′-triphosphate-gated ion channel P2X(2) receptor subunits in adult and developing rat cochlea. J Comp Neurol. 2000; 421:289–301. [PubMed: 10813788]
10. Robertson D. Horseradish peroxidase injection of physiologically characterized afferent and efferent neurones in the guinea pig spiral ganglion. Hear Res. 1984; 15:113–21. [PubMed: 6490538]

11. Jagger DJ, Housley GD. Membrane properties of type II spiral ganglion neurones identified in a neonatal rat cochlear slice. J Physiol. 2003; 552:525–33. [PubMed: 14561834]
12. Reid MA, Flores-Otero J, Davis RL. Firing patterns of type II spiral ganglion neurons in vitro. J Neurosci. 2004; 24:733–42. [PubMed: 14736859]
13. Goutman JD, Fuchs PA, Glowatzki E. Facilitating efferent inhibition of inner hair cells in the cochlea of the neonatal rat. J Physiol. 2005; 566:49–59. [PubMed: 15878942]
14. Thiers FA, Nadol JB Jr. Liberman MC. Reciprocal synapses between outer hair cells and their afferent terminals: evidence for a local neural network in the mammalian cochlea. J Assoc Res Otolaryngol. 2008; 9:477–89. [PubMed: 18688678]
15. Matsubara A, Laake JH, Davanger S, Usami S, Ottersen OP. Organization of AMPA receptor subunits at a glutamate synapse: a quantitative immunogold analysis of hair cell synapses in the rat organ of Corti. J Neurosci. 1996; 16:4457–67. [PubMed: 8699256]
16. Knirsch M, et al. Persistence of Ca(v)1.3 Ca^{2+} channels in mature outer hair cells supports outer hair cell afferent signaling. J Neurosci. 2007; 27:6442–51. [PubMed: 17567805]
17. Beurg M, et al. Calcium- and otoferlin-dependent exocytosis by immature outer hair cells. J Neurosci. 2008; 28:1798–803. [PubMed: 18287496]
18. Dunn RA, Morest DK. Receptor synapses without synaptic ribbons in the cochlea of the cat. Proc Natl Acad Sci U S A. 1975; 72:3599–603. [PubMed: 1059148]
19. Hashimoto S, Kimura RS. Computer-aided three-dimensional reconstruction and morphometry of the outer hair cells of the guinea pig cochlea. Acta Otolaryngol. 1988; 105:64–74. [PubMed: 3341163]
20. Simmons DD, Liberman MC. Afferent innervation of outer hair cells in adult cats: II. Electron microscopic analysis of fibers labeled with horseradish peroxidase. J Comp Neurol. 1988; 270:145–54. [PubMed: 3372736]
21. Burgess BJ, Adams JC, Nadol JB Jr. Morphologic evidence for innervation of Deiters' and Hensen's cells in the guinea pig. Hear Res. 1997; 108:74–82. [PubMed: 9213124]
22. Neef A, et al. Probing the mechanism of exocytosis at the hair cell ribbon synapse. J Neurosci. 2007; 27:12933–44. [PubMed: 18032667]
23. Berglund AM, Brown MC. Central trajectories of type II spiral ganglion cells from various cochlear regions in mice. Hear Res. 1994; 75:121–30. [PubMed: 8071139]
24. Huang LC, Greenwood D, Thorne PR, Housley GD. Developmental regulation of neuron-specific P2X3 receptor expression in the rat cochlea. J Comp Neurol. 2005; 484:133–43. [PubMed: 15736235]
25. Tritsch NX, Yi E, Gale JE, Glowatzki E, Bergles DE. The origin of spontaneous activity in the developing auditory system. Nature. 2007; 450:50–5. [PubMed: 17972875]
26. Brown MC, Liberman MC, Benson TE, Ryugo DK. Brainstem branches from olivocochlear axons in cats and rodents. J Comp Neurol. 1988; 278:591–603. [PubMed: 3230172]
27. Gale JE, Piazza V, Ciubotaru CD, Mammano F. A mechanism for sensing noise damage in the inner ear. Curr Biol. 2004; 14:526–9. [PubMed: 15043820]
28. Munoz DJ, Kendrick IS, Rassam M, Thorne PR. Vesicular storage of adenosine triphosphate in the guinea-pig cochlear lateral wall and concentrations of ATP in the endolymph during sound exposure and hypoxia. Acta Otolaryngol. 2001; 121:10–5. [PubMed: 11270486]
29. Burnstock G. Purinergic receptors and pain. Curr Pharm Des. 2009; 15:1717–35. [PubMed: 19442186]
30. Wang JC, et al. Noise induces up-regulation of P2X2 receptor subunit of ATP-gated ion channels in the rat cochlea. Neuroreport. 2003; 14:817–23. [PubMed: 12858039]

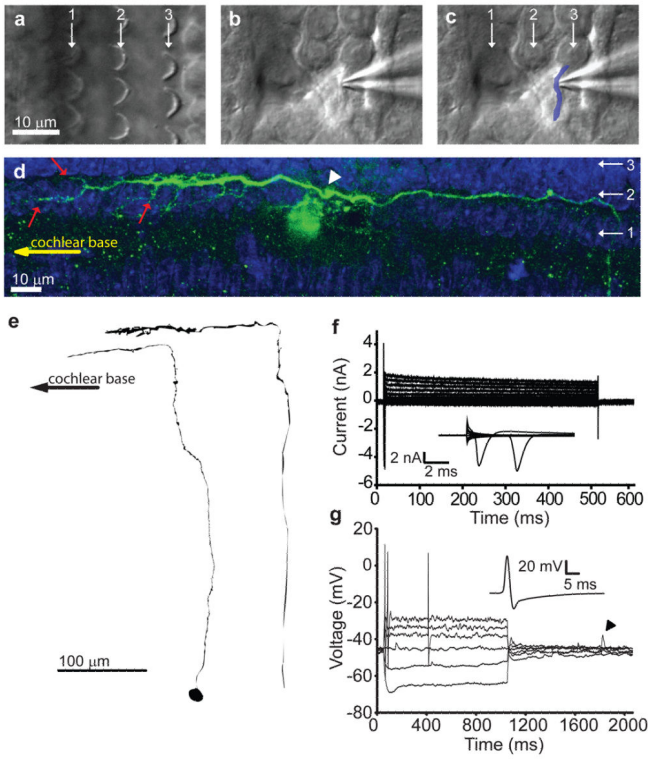

Figure 1.

Recording from Type II terminal arbors. a. OHC cilia (white arrows). b.-c. Pipette attached to Type II fiber below OHCs. d. Confocal projection of dye-filled fiber (green). OHC nuclei (blue, DAPI) visible in rows (1-3), arrows (red) indicate fiber branches toward OHCs. Recording site (white arrowhead) near dye artifact 'cloud'. e. Drawings of fill from (d) (P6, OHC row 2) and another fiber (P5, OHC row 1). f. Currents evoked by 10 mV steps from −80 mV. Inset: Selected inward currents, expanded. g. Current-clamp evoked action potentials (threshold: −32.1 ± 10.0 mV). Resting potential −56.9 ± 10.2 mV (n=10). Spontaneous action potential (inset) and small EPSPs (arrowhead). P5-9 rats.

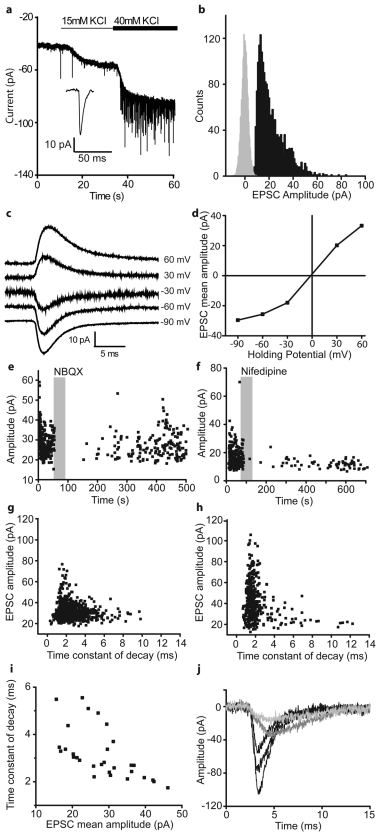

Figure 2.

Excitatory postsynaptic currents (EPSCs) in Type II fibers. a. Elevated extracellular potassium evoked EPSCs. Inset: EPSC waveform. b. Representative EPSC amplitude distribution (scaled noise in grey). c. Average EPSCs and d., resulting I-V relation. e. EPSC diary plot showing reversible block by NBQX (10 μM). f. EPSC diary plot showing reversible block by nifedipine (50 μM). g.-h. Amplitude versus decay time constant for EPSCs from two fibers. i. Mean decay time constant versus mean EPSC amplitude from 30 fibers. Linear regression fit ($F_{1,29}$=16.43, p=0.004; r^2=0.37) j. Exemplar EPSC waveforms (fiber in 'h'). P5-P9 rats.

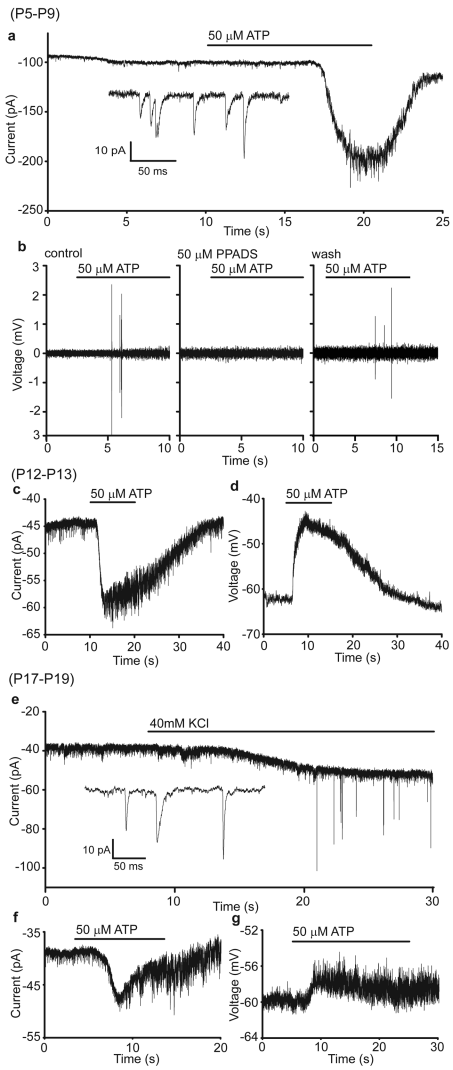

Figure 3.

ATP stimulates Type II fibers. a. ATP-evoked inward currents in postnatal (P5-9) fibers (142.7 ± 73.6 pA, n=6) and increased EPSC frequency. Inset: ATP (1 μM) induced EPSCs in another cell. b. PPADS reversibly blocked ATP-induced repetitive action potentials (loose-patch extracellular record). c. ATP induced inward current (29.9 ± 17.4 pA, n=5) and EPSCs in P12-13 fibers. d. ATP depolarized P12-13 fibers (12.6 ± 4.8 mV, n=4). e. 40 mM extracellular potassium induced EPSCs in a P18 fiber. Inset: expanded waveforms, same cell. f. ATP evoked inward currents in three of six P17-19 fibers (10.1 ± 3.6 pA, n=3). g. ATP depolarized P17-19 fibers (3.1 ± 0.2 mV, n=2).